IMPROVEMENT OF INTERIOR AND EXTERIOR ORIENTATION OF THE THREE LINE CAMERA HRSC WITH A SIMULTANEOUS ADJUSTMENT

Michael Spiegel

Photogrammetry and Remote Sensing, Technische Universität, München, 80333 Muenchen, Germany
spiegel@bv.tum.de, www.remotesensing-tum.de

WG I/2, WG III/2, WG III/4, WG III/5, and WG IV/3

KEY WORDS: Three line camera, interior orientation, exterior orientation, HRSC, combined adjustment

ABSTRACT

Since January 2004 the High Resolution Stereo Camera (HRSC) on board the ESA Mission Mars Express (MEX) is imaging the surface of planet Mars in color and stereoscopically in high resolution. As part of the entire data processing concept the Institute of Photogrammetry and GeoInformation (IPI) of the Leibniz Universität Hannover and the Department Photogrammetry and Remote Sensing (FPF) of the Technische Universität München are jointly responsible for the photogrammetric adjustment of the MEX-HRSC orientation data. This will be accomplished by registration of the HRSC data to the Mars Observer Laser Altimeter (MOLA) data of Mars Global Surveyor Mission using single strips or neighboring strips forming a block. With the result of the processing chain, high quality products such as Digital Terrain Models (DTMs), ortho-image mosaics and shaded reliefs can be derived from the imagery. In this paper the concept of simultaneous adjustment of interior and exterior orientation and results of photogrammetric point determination is described.

1 INTRODUCTION

The ESA mission Mars Express Mission (MEX) with the High Resolution Stereo Camera (HRSC) on board started the orbiting phase in January 2004. During the first three years more than 1400 stereo images were acquired.

The primary goal of the Photogrammetry and Remote Sensing (FPF) at the Technical University of Munich is to determine the exterior and interior orientation of HRSC orbiting planet Mars during Mars Express mission. In general, the classical photogrammetric point determination requires image coordinates of tie points, constant interior orientation, and ground control points (GCP). In case of HRSC on Mars Express tie points will be measured automatically in the images by means of image matching. Interior orientation is known from calibration. Observations for the exterior orientation will be derived from star observation, Inertial Measurement Unit (IMU) measurements, and doppler measurements. Unfortunately, these observations for the parameters of the exterior orientation will probably not be precise enough for a consistent photogrammetric point determination on a global level.

Additional control information is necessary in order to fit photogrammetrically derived object points into the existing reference system on Mars. On Mars there are only few precisely known points which can serve as classical GCPs. But there is a large number of ground points measured by MOLA. The characteristics of the laser points are, that they can not be identified in the images in an easy way. I.e., image coordinates of most of these points can not be measured, and therefore, it is not possible to treat them as normal GCPs in a bundle adjustment. As a remedy it is proposed to use control surfaces derived from the MOLA points.

2 DATA SOURCES

2.1 High Resolution Stereo Camera (HRSC)

The HRSC is a multi-sensor pushbroom camera consisting of nine Charge Coupled Device (CCD) line sensors for simultaneous high resolution stereo, multispectral, and multi-phase imaging. It has one panchromatic nadir channel, four panchromatic stereo channels, and four channels for color. The convergence angles between the nadir- and the stereo sensors are 21 and 14 gon. Figure 1 shows a HRSC Nadir image with tie points.

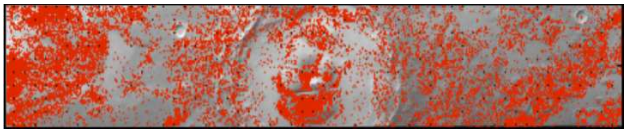

Figure 1: HRSC Nadir image with tie points(red)

The sensor arrays with 5184 active pixels each are arranged perpendicular to the direction of flight in one focal plane. The images are generated by catenating the continuously acquired line-images. The result is one image per sensor and orbit. One image strip includes all images of one orbit. The pixel size on ground of 12 m will be reached at an altitude of 270 km at pericentre and increase to 50 m at an altitude of 1000 km (Neukum and Hoffmann, 2000). At pericentre one image strip covers an area of about 60 km across trajectory. In general, the strip has a length of about 400 km up to 4000 km.

The three-dimensional position of the spacecraft is determined by the European Space Agency (ESA) applying a combination of doppler shift measurements (up to 15 times per orbit), acquisition of ranging data, triangulation measurements, and orbit analysis. The orbit accuracy at the pericentre is given as an interval of

maximum and minimum accuracy for the whole mission duration (Hechler and Yáñez, 2000). In direction of flight, perpendicular to the direction of flight, and radial direction the accuracy of the orbit is assumed to be about 1000 m.

The attitude of the spacecraft is commanded by European Space Operation Center (ESOC). With this predicted attitude, the orbiter adjusts itself using measurements of star tracker cameras and from an Inertial Measurement Unit (IMU). But, for photogrammetric point determination only the predicted attitude is available. Therefore, the accuracy of the nadir pointing results from a combination of attitude errors and navigation errors. The values for accuracies are 25 mdeg for all three rotation angles φ (pitch), ω (roll), and κ (yaw) (Astrium, 2001).

2.2 Mars Observer Laser Altimeter (MOLA)

In February 1999 the Mars Global Surveyor (MGS) spacecraft entered the mapping orbit at Mars. During the recording time (February 1999 to June 2001) the MOLA instrument acquired more than 640 million observations by measuring the distances between the orbiter and the surface of Mars. In combination with orbit and attitude information these altimeter measurements have been processed to coordinates of object points on the ground. Therefore, each orbit results in one track of MOLA points (Smith et al., 2001).

In addition to the surface described by the original, irregularly spaced MOLA track points, NASA (Neumann et al., 2003) distributed a grid-based global Digital Terrain Model (DTM) which is derived from these MOLA points (see Figure 2). The accuracy of DTM is 200 m in planimetry and 10 m in height.

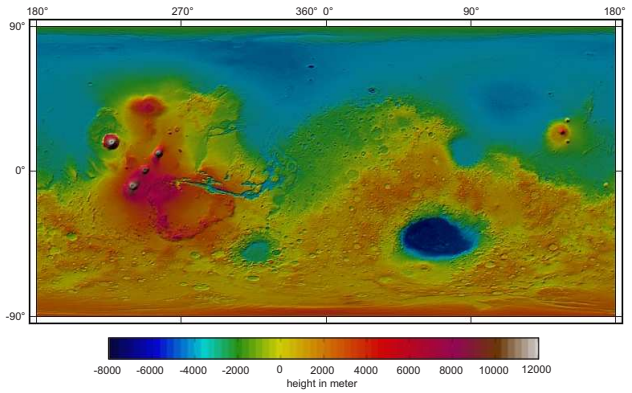

Figure 2: MOLA DTM

3 CONCEPT

In this Section the concept of automated measurement of image coordinates of tie points and the bundle adjustment will be described.

3.1 Matching

For automatic extraction of image coordinates of tie points software *hwmatch1* is used. Originally, *hwmatch1* was developed at the FPF in Munich for frame images. The IPI implement in *hwmatch1* the extended functional model for three line imagery (Ebner et al., 1994) and modified the software according to the requirements of the Mars Express Mission (Heipke et al., 2004, Schmidt et al., 2005).

As input data the matching needs images, the observed exterior orientation, and the calibrated interior orientation parameters. As an optional input it is possible to use a MOLA DTM as approximate information.

The matching uses feature based techniques. Point features are extracted of the entire images using the Förstner operator. The images of all sensors are matched pairwise in all combinations using the cross correlation coefficient as similarity measure. The results of pixel correlations are sets of image coordinates of tie points for each image. In addition, the results are refined step by step through different levels of image pyramids. To optimize the results of lowest image pyramid, a Multi Least Image Squares Matching (MI-LSM) is used.

3.2 Mathematical model of bundle adjustment

In the bundle adjustment the concept of orientation points proposed by (Hofmann et al., 1982) is used. This approach estimates the parameters of the exterior orientation only at a few selected image lines, at the so-called orientation points. Additional DTM data as control information is used to fit photogrammetrically derived object points into the existing reference system on Mars.

3.2.1 Collinearity equations. The mathematical model for photogrammtric point determination with a three-line camera is based on the well known collinearity equations. These equations describe the fundamental geometrical condition that the rays through the three corresponding image points and the corresponding perspective centers intersect in the object point P_i (see Figure 3).

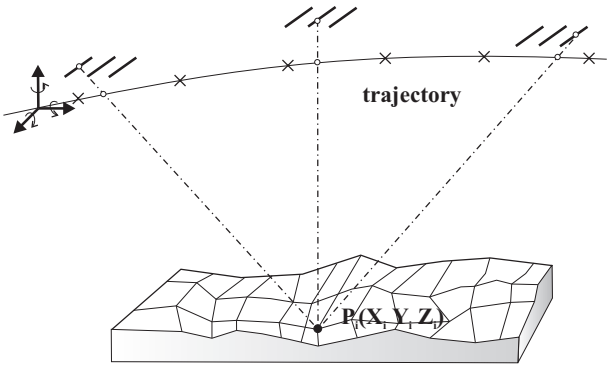

Figure 3: Imaging principle with three line camera

Two collinearity equations (Equation (1)) are established for each observed image coordinate pair. For every object point P_i there are several equations, because observed image coordinates are found in images of different sensors s.

$$
\begin{aligned}
& x_{ij_s} + \hat{x}_{0_s} + \hat{v}_{x_{ij_s}} = \\
& = c\,\frac{\hat{r}_{j11}(\hat{X}_i - \hat{X}_j) + \hat{r}_{j21}(\hat{Y}_i - \hat{Y}_j) + \hat{r}_{j31}(\hat{Z}_i - \hat{Z}_j)}{\hat{r}_{j13}(\hat{X}_i - \hat{X}_j) + \hat{r}_{j23}(\hat{Y}_i - \hat{Y}_j) + \hat{r}_{j33}(\hat{Z}_i - \hat{Z}_j)} \\
& y_{ij_s} + \hat{y}_{0_s} + \hat{v}_{y_{ij_s}} = \\
& = c\,\frac{\hat{r}_{j11}(\hat{X}_i - \hat{X}_j) + \hat{r}_{j21}(\hat{Y}_i - \hat{Y}_j) + \hat{r}_{j31}(\hat{Z}_i - \hat{Z}_j)}{\hat{r}_{j13}(\hat{X}_i - \hat{X}_j) + \hat{r}_{j23}(\hat{Y}_i - \hat{Y}_j) + \hat{r}_{j33}(\hat{Z}_i - \hat{Z}_j)}
\end{aligned}
\tag{1}
$$

with

x_{ij_s}, y_{ij_s}	:	observed image coordinates of object point
$\hat{v}_{x_{ij_s}}, \hat{v}_{y_{ij_s}}$	:	residuals of image coordinates
$\hat{X}_i, \hat{Y}_i, \hat{Z}_i$	:	coordinates of object point P_i
$\hat{X}_j, \hat{Y}_j, \hat{Z}_j$	:	coordinates of projective center
$\hat{r}_{j11}, .., \hat{r}_{j33}$	:	elements of rotation matrix (Spiegel, 2007)
$\hat{x}_{0_s}, \hat{y}_{0_s}$	:	unknown parameters of interior orientation
c	:	constant parameter of interior orientation

Generally, the collinearity equations are formulated for each pair of image coordinates. Therefore, it is necessary to improve the exterior parameters for each image line in which observed image coordinates are available. But, this is not possible due to geometric reasons. In the case of Mars Express (satellite Orbit) the trajectory is assumed to stable and the parameters of the exterior orientation are improved only at few selected positions m (orientation points). But, for all collinearity equations the exterior orientation parameters are needed. Therefore, the parameters of exterior orientation ($\hat{X}_j$, $\hat{Y}_j$, $\hat{Z}_j$, $\hat{\varphi}_j$, $\hat{\omega}_j$, $\hat{\kappa}_j$) laying between the orientation are formulated with Lagrange polynomials of grade three (Spiegel, 2007).

3.2.2 Observed unknowns. In the case of Mars Express, there are observed parameters of exterior orientation of each image line. At the orientation points m these observations can introduced into the adjustment with additional observation equations (Equation (2)).

$$\begin{aligned} \hat{v}_{X_m} &= \hat{X}_m - X_m \\ \hat{v}_{Y_m} &= \hat{Y}_m - Y_m \\ \hat{v}_{Z_m} &= \hat{X}_m - Z_m \\ \hat{v}_{\varphi_m} &= \hat{\varphi}_m - \varphi_m \\ \hat{v}_{\omega_m} &= \hat{\omega}_m - \omega_m \\ \hat{v}_{\kappa_m} &= \hat{\kappa}_m - \kappa_m \end{aligned} \tag{2}$$

with

$\hat{v}_{X_m}, .., \hat{v}_{\kappa_m}$	:	residuals at exterior orientation points m
$\hat{X}_m, .., \hat{\kappa}_m$	:	unknown exterior orientation parameters
	:	at orientation points m
$X_m, .., \kappa_m$	:	observed exterior orientation parameters
	:	at orientation points m

To avoid interpolation problems, constant differences (δX_j, δY_j, δZ_j, $\delta\varphi_j$, $\delta\omega_j$, $\delta\kappa_j$) should be added to the exterior orientation parameters ($\hat{X}_j$, $\hat{Y}_j$, $\hat{Z}_j$, $\hat{\varphi}_j$, $\hat{\omega}_j$, $\hat{\kappa}_j$) at the image lines j between the orientation points (Spiegel, 2007).

3.2.3 Systematic effects in parameter of exterior orientation. The three-dimensional position of the spacecraft is determined by ESA up to 15 times per orbit. Because of doppler shift measurements there are systematic effects in observed exterior orientation (see Section 2.1). To model these effects in bundle adjustment it is possible to use additional bias (offset) and drift parameters. For this, it is necessary to expand equation (2) with bias and drift parameters (Equation (3)).

$$\begin{aligned} \hat{v}_{X_m} &= \hat{X}_m - X_m + \hat{X}_B + j\,\hat{X}_D \\ \hat{v}_{Y_m} &= \hat{Y}_m - Y_m + \hat{Y}_B + j\,\hat{Y}_D \\ \hat{v}_{Z_m} &= \hat{Z}_m - Z_m + \hat{Z}_B + j\,\hat{Z}_D \end{aligned} \tag{3}$$

with

$\hat{v}_{X_m}, .., \hat{v}_{Z_m}$	:	residuals at exterior orientation points m
$\hat{X}_m, .., \hat{Z}_m$	:	unknown exterior orientation parameters
	:	at orientation points m
$X_m, .., Z_m$	:	observed exterior orientation parameters
	:	at orientation points m
$\hat{X}_B, .., \hat{Z}_B$	:	unknown bias
$\hat{X}_D, .. \hat{Z}_D$	:	unknown drift
j	:	number of image line

Also, additional observation equations for bias and drift has to be introduced (Equation (4)).

$$\begin{aligned} \hat{v}_{X_B} &= \hat{X}_B - X_B \\ \hat{v}_{X_D} &= \hat{X}_D - X_D \\ \hat{v}_{Y_B} &= \hat{Y}_B - Y_B \\ \hat{v}_{Y_D} &= \hat{Y}_D - Y_D \\ \hat{v}_{Z_B} &= \hat{Z}_B - Z_B \\ \hat{v}_{Z_D} &= \hat{Z}_D - Z_D \end{aligned} \tag{4}$$

with

$\hat{v}_{X_B}, .., \hat{v}_{Z_B}$	:	residuals of bias
$\hat{X}_B, .., \hat{Z}_B$	:	unknown bias
$X_B, .., Z_B$	:	observed bias
$\hat{v}_{X_B}, .., \hat{v}_{z_B}$	:	residuals of drift
$\hat{X}_D, .., \hat{Z}_D$	:	unknown drift
$X_D, .., Z_D$	:	observed drift

ESOC is distributing predicted attitude values of the spacecraft (see Section 2.1). Thus, it is not necessary to formulate additional equations to consider systematic effects in the attitude angles.

3.2.4 Interior orientation. To adjust parameters of interior orientation, two observation equations per sensor are introduced in the bundle adjustment (Equation (5)).

$$\begin{aligned} \hat{v}_{x_{0_s}} &= \hat{x}_{0_s} - x_{0_s} \\ \hat{v}_{y_{0_s}} &= \hat{y}_{0_s} - y_{0_s} \end{aligned} \tag{5}$$

with

$\hat{v}_{x_{0_s}}, \hat{v}_{y_{0_s}}$	:	residuals of parameter of interior orientation
$\hat{x}_{0_s}, \hat{y}_{0_s}$	:	unknown parameters of interior orientation
x_{0_s}, y_{0_s}	:	observations of parameter of interior orientation
s	:	sensor

3.2.5 MOLA DTM as control information. Starting point of this discussion about DTM data as control information is the approach of (Strunz, 1993). This approach describes the use of DTM as additional or exclusive control information for aerial triangulation. Transferring this approach to the case of Mars Express and HRSC means that, the control information is the surface defined by MOLA DTM and HRSC points lie on these surfaces. A drawback of this approach is that it does not use the original MOLA track points but interpolated DTM points. The advantage of this approach is that the effort to search for adequate neighboring MOLA points is reduced because the DTM has a regular grid structure.

This approach uses a least squares adjustment with additional conditions to get a relation between a DTM and the HRSC points. As already mentioned, the HRSC points have to lie on a bilinear surface defined by four neighboring MOLA DTM points, which enclose the HRSC point (see Figure 4). This condition can be formulated as a constraint on the vertical distance from the HRSC point to the bilinear surface. Furthermore, this constraint can be substituted by a fictive observation, used as additional observation in the bundle adjustment.

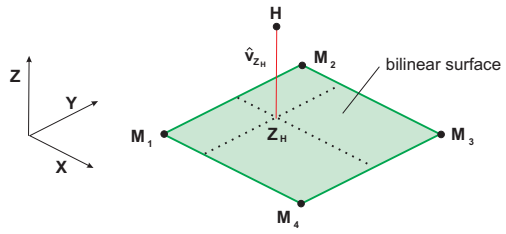

Figure 4: Fitting HRSC point in bilinear surface defined by MOLA DTM

The functional model has to be extended with an additional observation equation per object point (Equation (6)).

$$\hat{v}_{Z_H} = \hat{Z}_H - Z_H \tag{6}$$

with

$\hat{v}_{Z_H}$: residuals of height $\hat{Z}_H$
$\hat{Z}_H$: unknown height of object point H
Z_H : fictive observation

The fictive observation Z_H for one object point is generated by bilinear interpolation of the MOLA surface (M_1, M_2, M_3, M_4) at the point of the unknown object points $\hat{X}_H, \hat{Y}_H$ (Equation (7)).

$$\begin{aligned} Z_H = & [(1 - \tfrac{\hat{X}_H - X_{M_1}}{d})(1 - \tfrac{\hat{Y}_H - Y_{M_1}}{d})\ Z_{M_1} + \\ & + (\tfrac{\hat{X}_H - X_{M_1}}{d})(1 - \tfrac{\hat{Y}_H - Y_{M_1}}{d})\ Z_{M_4} + \\ & + (1 - \tfrac{\hat{X}_H - X_{M_1}}{d})(\tfrac{\hat{Y}_H - Y_{M_1}}{d})\ Z_{M_2} + \\ & + (\tfrac{\hat{X}_H - X_{M_1}}{d})(\tfrac{\hat{Y}_H - Y_{M_1}}{d})\ Z_{M_3}] \end{aligned} \tag{7}$$

with

Z_H : fictive observation
$\hat{X}_H, \hat{Y}_H$: unknown coordinates of object points H
$X_{M_i}, Y_{M_i}, Z_{Z_i}$: constant coordinates of MOLA DTM mesh points
d : mesh width of MOLA DTM $(d = X_{M_4} - X_{M_1} = Y_{M_2} - Y_{M_1})$

With this approach an improvement of the height (Z) can be expected, of course. An improvement in planimetry (X, Y) can only be determined, if there are different local terrain slopes at the different MOLA surfaces (Ebner and Ohlhof, 1994). Figure 5(a) shows a situation before bundle adjustment. After bundle adjustment, the differences between HRSC points and MOLA DTM are reduced (see Figure 5(b)).

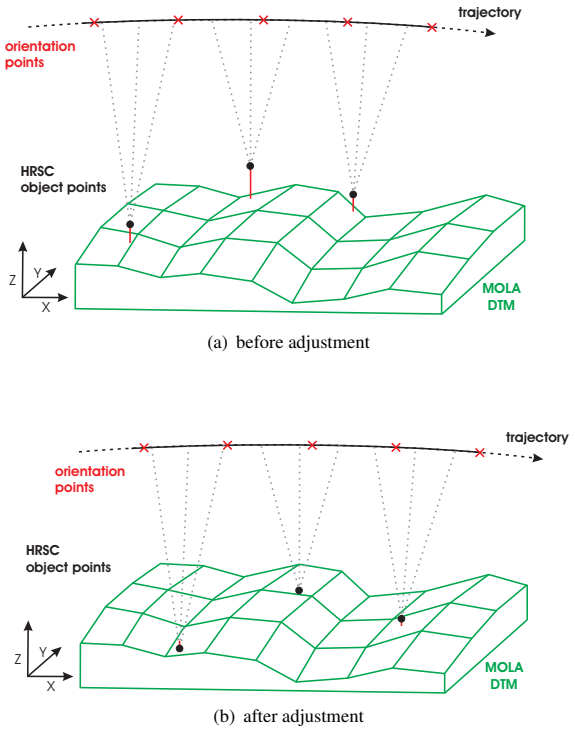

(a) before adjustment

(b) after adjustment

Figure 5: MOLA as control information

4 INTERIOR ORIENTATION

An investigation shows, that the parameters $\hat{x}_{0_s}$ and $\hat{y}_{0_s}$ of interior orientation can be improved for 7 of 9 lines. Therefore, two observation equations per sensor (=14 total) are introduced in the bundle adjustment. The other parameters of interior orientation are constant in adjustment.

For improvement of interior orientation, 46 orbits with good imaging conditions are selected. For all orbits the parameters $\hat{x}_{0_s}$ and $\hat{y}_{0_s}$ of nadir and the two stereo channels S1 and S2 are improved. For a part of selected orbits the color lines are not available in adequate geometric resolution. Therefore, the color lines can be improved only for 17 orbits. Afterwards the mean values for all orbits are computed and only one new set of interior orientation parameters is created.

Systematic residuals at the image coordinates of one orbit before adjustment of interior orientation is shown in figure 6. In the figure, each sensor is divided in 8 parts. For these parts the root mean square error is shown.

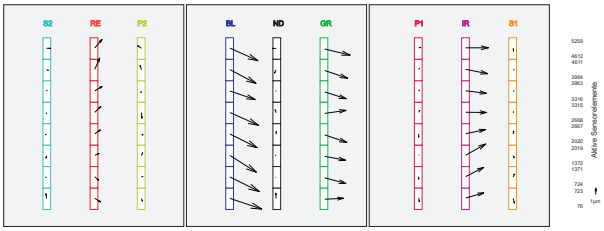

Figure 6: Residuals of image coordinates of orbit h2063 before adjustment of interior orientation

With new interior orientation, the residuals at image coordinates are reduced and there are no longer systematic residuals in the image coordinates (see Figure 7) compared to the case without new interior orientation.

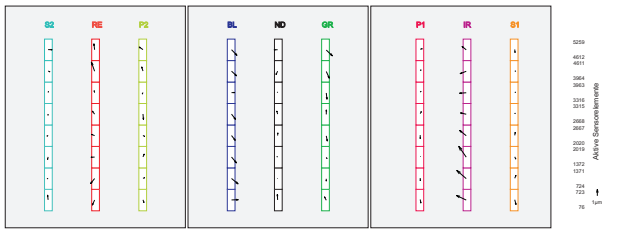

Figure 7: Residuals of image coordinates of orbit h2063 after adjustment of interior orientation

A comparison of Z-differences between HRSC object points and MOLA DTM shows the advantage of this approach. Certainly, the differences using calibrated interior orientation is better than without any bundle adjustment. But, the results can be improved with the new interior orientation.

5 RESULTS OF PROCESSING HRSC IMAGERY

In this section, the results of the bundle adjustment using the new interior orientation (considered to be stable) will be discussed for three cases: Using the nominal exterior orientation (Case A): Figure 8(a) shows the average displacements in planimetry between neighboring strips. The average displacements are in the range of 150 m up to 200 m in planimetry. The height differences between the HRSC object points and the MOLA DTM are irregularly distributed over the whole area (see Figure 8(b)).

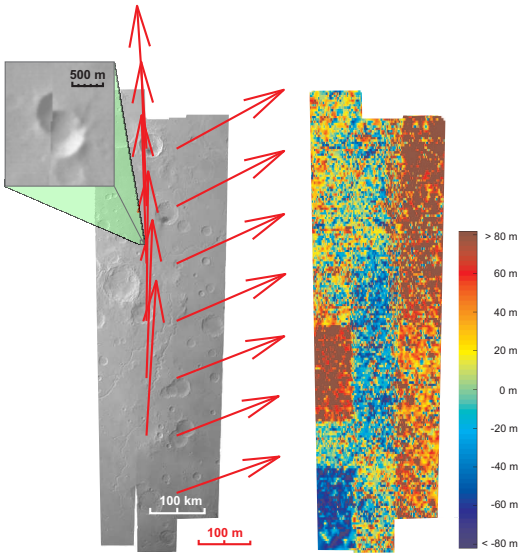

(a) planimetry (X/Y) (b) height diff. (ΔZ)

Figure 8: results before bundle adjustment

Improved exterior orientation with single strips (Case B): The Figure 9(a) shows the average displacements between strips, again. But, in this case the average displacements are smaller (only 15 m up to 40 m) as in case A. Also, the height differences are much smaller as in the case discussed before (see Figure 9(b)).

Improved exterior orientation adjusted in a block (Case C): The best results are achieved in this case. The average displacements in planimetry are lower than 10 m (Figure 10(a)). The improvement of the height differences between the HRSC object points and the MOLA DTM (see Figure 10(b)) is in this case only small because of the very good results in case B.

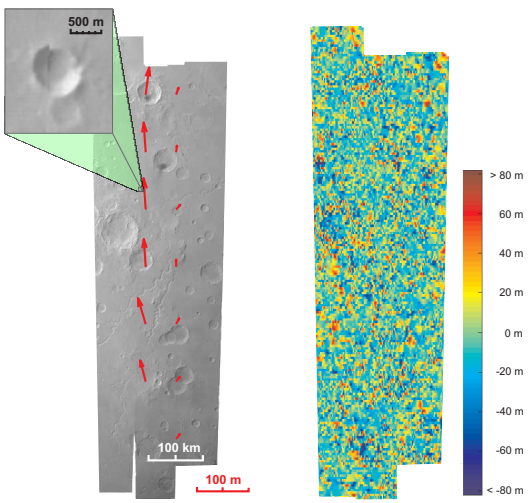

(a) planimetry (X/Y) (b) height diff. (ΔZ)

Figure 9: results of adjustment as single strip

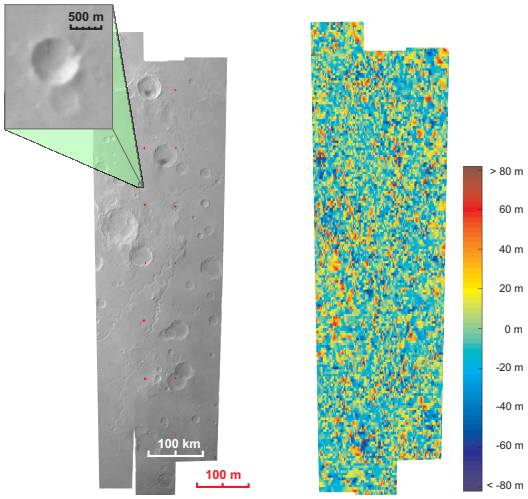

(a) Adjustment as block (b) height diff. (ΔZ)

Figure 10: results of adjustment in a block

6 CONCLUSION

The parameter of exterior and interior orientation can be improved by using bundle adjustment. Regarding to interior orientation, a reduction of residuals at the image coordinates after bundle adjustment can be reached. Also, the Z-differences between HRSC object points and MOLA DTM is reduced for all 1200 investigated orbits with the new interior orientation, more or less. Therefore, it is absolutely necessary to use the new interior orientation in further investigations.

Using new interior orientation by computing single strips or blocks with bundle adjustment, the best result is reached with the bundle adjustment of a block. But also, the adjustment of single strips leads to good results. Finally, there are a high consistency between HRSC points and MOLA DTM, which constitutes the valid reference system on Mars.

REFERENCES

Astrium, 2001. Mars Express – System Requirements Specification. Technical Report MEX.MMT.TN.0519, Astrium.

Ebner, H. and Ohlhof, T., 1994. Utilization of Ground Control Points for Image Orientation without Point Identification in Image Space. In: International Archives of Photogrammetry and Remote Sensing, Vol. 30, Part 3/1, pp. 206–211.

Ebner, H., Kornus, W. and Ohlhof, T., 1994. A Simulation Study on Point Determination for the MOMS-02/D2 Space Project using an Extended Functional Model. In: Geo-Informations-Systeme, pp. 11–16.

Ebner, H., Spiegel, M., Giese, A. B. B., Neukum, G. and the HRSC Co-Investigator Team, 2004. Improving the Exterior Orientation of Mars Express HRSC Imagery. In: International Archives of Photogrammetry and Remote Sensing, Vol. 35 (B4), pp. 852–857.

Hechler, M. and Yáñez, A., 2000. Mars Express – Consolidated Report on Mission Analysis Issue 2.0. Technical Report MEX-ESC-RP-5500, ESA.

Heipke, C., Schmidt, R., Oberst, J., Neukum, G. and the HRSC Co-Investigator Team, 2004. Performance of Automatic Tie Point Extraction Using HRSC Imagery of Mars Express Mission. In: International Archives of Photogrammetry and Remote Sensing, Vol. 35 (B4), pp. 846–851.

Hofmann, O., Navé, P. and Ebner, H., 1982. DPS - A Digital Photogrammetric System for Producing Digital Elevation Models and Orthophotos by Means of Linear Array Scanner Imagery. In: International Archives of Photogrammetry and Remote Sensing, Vol. 24-III, pp. 216–227.

Neukum, G. and Hoffmann, H., 2000. Images of Mars. In: R. Pellinen and P. Raudsepp (eds), Towards Mars!, pp. 129–152.

Neumann, G., Lemoine, F., Smith, D. and Zuber, M., 2003. The Mars Orbiter Laser Altimeter Archive: Final Precision Experiment Data Record Release and Status of Radiometry. In: Lunar and Planetary Science XXXIV, Abstract #1978, Lunar and Planetary Institute, Houston (CD-ROM).

Schmidt, R., Heipke, C., Brand, R., Neukum, G. and the HRSC Co-Investigator Team, 2005. Automatische Bestimmung von Verknüpfungspunkten in HRSC-Bildern der Mars Express Mission. In: Photogrammetrie Fernerkundung Geoinformation, E. Schweizerbart'sche Verlagsbuchhandlung, Stuttgart, pp. 373–379.

Smith, D., Zuber, M., Frey, H., Garvin, J., Head, J., Muhleman, D., Pettengill, G., Phillips, R., Solomon, S., Zwally, H., Banerdt, W., Duxbury, T., Golombek, M., Lemoine, F., Neumann, G., Rowlands, D., Aharonson, O., Ford, P., Ivanov, A., Johnson, C., McGovern, P., Abshire, J., Afzal, R. and Sun, X., 2001. Mars Orbiter Laser Altimeter: Experiment Summary After the First Year of Global Mapping of Mars. In: Journal of Geophysical Research, Vol. 106(E10), pp. 23,689–23,722.

Spiegel, M., 2007. Kombinierte Ausgleichung der Mars Express HRSC Zeilenbilddaten und des Mars Global Surveyor MOLA DGM. Technische Universität München, http://nbn-resolving.de/urn/resolver.pl?urn:nbn:de:bvb:91-diss-20070801-618406-1-4.

Spiegel, M., Stilla, U., Giese, B., Neukum, G. and the HRSC Co-Investigator Team, 2005. Bündelausgleichung von HRSC-Bilddaten mit Mars Observer Laser Altimeter-Daten als Passinformation. In: Photogrammetrie Fernerkundung Geoinformation, E. Schweizerbart'sche Verlagsbuchhandlung, Stuttgart, pp. 381–386.

Strunz, G., 1993. Bildorientierung und Objektrekonstruktion mit Punkten, Linien und Flächen. Dissertationsschrift, DGK-C, Nr. 408, Deutsche Geodätische Kommission, München.

ACKNOWLEDGEMENTS

The author thank the HRSC Experiment Teams at DLR Berlin and Freie Universitaet Berlin as well as the Mars Express Project Teams at ESTEC and ESOC for their successful planning and acquisition of data as well as for making the processed data available to the HRSC Team. The authors acknowledge the effort of Ralph Schmidt, Christian Heipke, Heinrich Ebner, Uwe Stilla, and Gerhard Neukum who have contributed to this investigation in the preparatory phase and in scientific discussions within the Team.

This work is funded by Deutsches Zentrum für Luft- und Raumfahrt e.V. (DLR) under grant no. 50 QM 0103. This support is gratefully acknowledged.